Supporting Information

Carbon dots boost nitrate-to-ammonia conversion via hydrogen evolution control in CDs/Ag nanocomposites

Chan Wang[a], Huan Zhuo[a], Wenchao Zhang[b], Dongliang Xiang[c], Jiace Hao[a], Qijun Song[a], Han Zhu*[a]

a. Key Laboratory of Synthetic and Biological Colloids, Ministry of Education, School of Chemical and Material Engineering, Jiangnan University, Wuxi, Jiangsu 214122, P. R. China. E-mail: zhysw@jiangnan.edu.cn.

b. School of Chemistry and Life Sciences, Suzhou University of Science and Technology, Suzhou, 215009, Jiangsu, P. R. China.

c. Jiangsu Snow Leopard Daily Chemical Co. Ltd, Wuxi, Jiangsu, 214400, P. R. China.

1. Experimental Section

1.1. Materials

Catechol, urea, N'N-dimethylformamide (DMF), silver nitrate ($AgNO_3$), polyvinylpyrrolidone (PVP), ethanol (C_2H_5OH), potassium hydroxide (KOH), potassium nitrate (KNO_3), potassium nitrite (KNO_2), sodium hydroxide (NaOH), sodium citrate dihydrate, salicylic acid, 4-aminobenzenesulfonamide, hydrochloric acid (HCl), N-(1-naphthyl) ethylenediamine dihydrochloride and ammonium chloride (NH_4Cl) were purchased from Sinopharm Chemical Reagent Co., Ltd. Sodium hypochlorite pentahydrate ($NaClO{\cdot}5H_2O$), sodium nitroferricyanide dehydrate ($C_5FeN_6Na_2O{\cdot}2H_2O$) and potassium nitrate-$^{15}N$ ($K^{15}NO_3$) were purchased from Macklin Co., Ltd. Dimethyl sulfoxide (DMSO) was obtained from Cambridge Isotope Laboratories, Inc. 4-Dimethylaminobenzaldehyde ($C_9H_{11}NO$) was acquired by Sigma-Aldrich. All chemical reagents were analytic grades and used without further purification. Argon (Ar, 99.999 %) were bought from Xinxiyi Technology Co., Ltd (Jiangsu, China). Ultrapure water was used to prepare the aqueous solution. The anion exchange membrane (FAA-3-PK-130) was purchased from Suzhou Sinero Technology Co., Ltd.

1.2. Preparation of catalysts

1.2.1. Preparation of CDs

1 g of catechol and 0.33 g of urea were weighed respectively, dissolved in 10 mL of deionized water, mixed well and poured into a 25 mL polytetrafluoroethylene reactor, and kept warm at 200 ℃ for 6 h. At the end of the reaction, after the reactor was cooled down to room temperature, the synthesized solution was dialyzed with a dialysis bag of 1000 Da for 24 h (with the water changed once every 12 h). After dialysis, the solid powder of CDs was obtained by freeze-drying.

1.2.2. Preparation of CDs/Ag

CDs/Ag was synthesized by using a slight modification of a previous report. Briefly, 14.3 mg

of $AgNO_3$, 250 mg of PVP and 10 mg of CDs were dissolved in 8 mL of DMF, sonicated until completely dissolved, and then poured into a 25 mL reactor, which was kept warm at 150 ℃ for 5 h. When the reaction was finished, it was centrifuged and alcohol washed and dried to obtain CDs/Ag. Without the addition of CDs, the same steps were synthesized for the comparison sample AgNPs.

The synthesis method of CDs/Ag-5/15 is similar to CDs/Ag, except for the different amounts of CDs, which are 5 mg and 15 mg, respectively.

1.3. Characterization

Scanning electron microscopy (SEM) and transmission electron microscopy (TEM) images were captured by Hitachi S-4800 FE - SEM and JEOL JEM 2100 Olus electron microscope (Japan Electron Optics Laboratory Co., Ltd.). High-angle annular dark-field scanning transmission electron microscopy (HAADF - STEM) and energy dispersive X-ray analysis were performed on a FEI ThemisZ. Powder X-ray diffraction (XRD) data was obtained using Bruker D8 Advance X-ray diffractometer. The diffraction patterns from 10° to 90° were recorded in steps of 0.05°/s. X-ray photoelectron spectroscopy (XPS) measurements were carried out on Axis Supra electron spectrometer (Shimadzu, Japan) using Al Kα radiation of 600 W. Fourier-transform infrared (FT - IR) spectra were obtained by Nicolet 6700 spectrograph (Thermo Fisher Scientific, America). Thermogravimetric analysis (TGA) was performed using Mettler Toledo TGA 1100SF thermogravimetric analyzer (Mettler Toledo, Switzerland). The ultraviolet-visible (UV - Vis) absorbance spectra were measured on PERSEE TU-1950.

1.4. Electrochemical measurements

Electrochemical measurements were carried out at room temperature in a H-type electrolytic cell separated by an anion exchange membrane. The electrochemical responses were recorded using an Autolab electrochemical workstation. Carbon paper loaded with catalyst, Hg/HgO electrode and platinum mesh were used as working electrode, reference electrode and counter electrode, respectively. All potentials in this study were measured based on the Hg/HgO electrode and converted to the RHE reference scale by E (V vs RHE) = E (V vs Hg/HgO) + 0.0591 pH + 0.098. The working electrode was prepared as follows: 1 mg of CDs/Ag catalyst powder, 100 µl of ethanol, 5 µl of Nafion solution (Sigma Aldrich, 5 wt%) were mixed and ultrasound for at least 30 minutes to form a homogeneous ink. Then we used spray gun to spray the catalyst ink onto 1 cm × 1 cm carbon paper. For electrocatalytic NO_3^- reduction, solution containing 0.1 M KOH and 0.1 M KNO_3 was used as the electrolyte, unless otherwise stated, and uniformly distributed into the cathode and anode chambers. The electrolyte volume in both parts of the H-cell was 40 mL, and the electrolyte was purged with high-purity Ar prior to the measurements. The LSV was carried out at a scan rate of 5 mV/s. The potential-static test was performed at different potentials for 1 h. During the experiment, high-purity Ar was continuously injected into the cathode chamber. After electrolysis, the electrolyte was analyzed by UV-Vis spectrophotometry. Then, the next cycle of constant potential test was performed under the same conditions using fresh electrolyte.

1.5. Calculation of Faradaic efficiency and yield rate of NH_3

The yield rate of NH_3 (Y_{NH3}) can be calculated using the following formula: $Y_{NH3} = (C_{NH3} \times V) / (A \times t)$. The Faraday efficiency of NH_3 (FE_{NH3}) is the percentage of the charge consumed for NH_3 generation in the total charge and is calculated according to the following formula: $FE_{NH3} = (8 \times F \times C_{NH3} \times V) / Q$, where C_{NH3} is the measured concentration of NH_3 (µmol/mL), V is the volume of the electrolyte (40 mL); t is the electrolysis time (1 h); A is the geometric area of the electrode (1 cm^2);

F is the Faraday constant (96485 C/mol); and Q (C) is the total charge passing through the electrode and is the integral of the chronoamperometry curve.

1.6. Determination of NH_3

The concentration of NH_3 product was spectrophotometrically detected by the standard indophenol blue indicator method. Briefly, 2 mL diluted electrolyte, 2 mL solution A (1 M NaOH solution with 5 wt% sodium citrate and 5 wt% salicylic acid), 1 mL 0.05 M NaClO and 0.2 mL 1 wt% sodium nitroferricyanide (Ⅲ) dihydrate ($C_5FeN_6Na_2O{\cdot}2H_2O$) solution were mixed. After standing in the dark for 2 h, the absorption intensity at a wavelength of 655 nm was recorded by UV-Vis. For the quantitative determination of the amount of NH_3, a series of standard NH_4Cl solutions were used to calibrate the concentration-absorbance standard curve.

1.7. Determination of NO_2^-

First, 0.5 g of 4-aminobenzenesulfonamide was added to 50 mL of 10 wt % hydrochloric acid aqueous solution as color developer B, and 1 g/L of N-(1-naphthalenyl) ethylenediamine dihydrochloride aqueous solution as color developer C. Then, 100 μL color developer B and 100 μL color developer C were respectively added to 2 mL diluted electrolyte. After standing for 20 min, the absorption intensity at a wavelength of 540 nm was recorded by UV-Vis. For the quantitative of the amount of NO_2^-, a series of standard KNO_2 solutions were used to calibrate the concentration-absorbance standard curve.

1.8. Determination of NO_3^-

First, 50 μL of electrolyte was taken out from the cathode chamber and diluted to 5 mL. Then, 1 mL 1 M HCl and 0.1 mL sulfamic acid solution (0.8 wt%) were added to the above solution. After standing for 30 min, the absorption intensity at wavelengths of 220 nm and 275 nm were recorded by UV-Vis. Calculate the final absorbance value using the following equation: $A = A_{220nm}-2A_{275nm}$. For the quantitative of the amount of NO_3^-, a series of standard KNO_3 solutions were to calibrate the concentration-absorbance standard curve.

1.9. ^{14}N and ^{15}N ^1H NMR measurements

^1H NMR was recorded on an AVANCE Ⅲ HD 400 MHz system. After chronoamperometry measurements using $K^{14}NO_3$ - ^{14}N and $K^{15}NO_3$ - ^{15}N as nitrogen source in electrolyte respectively, 500 μL electrolyte was taken out, and 150 μL 1 M H_2SO_4 solution was added to adjust the pH, and 50 μL DMSO quantified by ^1H NMR at 400 Hz.

1.10. In situ Raman spectroscopy

In situ Raman measurements were performed jointly by the Raman microscope (Renishaw Trading Company Ltd, λ excited = 532 nm) and a CHI 660 electrochemical workstation. A hound home-made electrolyzer with Ag/AgCl electrode and platinum wire as the counter and reference electrode respectively was used to measure. The test was performed over a range of 800~2000 cm^{-1} during the chronoamperometry measurements from 0.21 V to -0.58 V vs RHE, and the dwell time at each potential was 3 minutes.

1.11. In situ FT-IR spectroscopy

In situ FT-IR measurements were performed jointly by the FT-IR microscope (Nicolet iS50) and a CHI 660 electrochemical workstation. Electrocatalytic nitrate reduction to ammonia was carried out in an electrolyte of 0.1 M KOH + 0.1 M KNO_3. After deducting the background, the in situ FT-IR spectra were measured from -0.57 V to -1.07 V vs RHE.

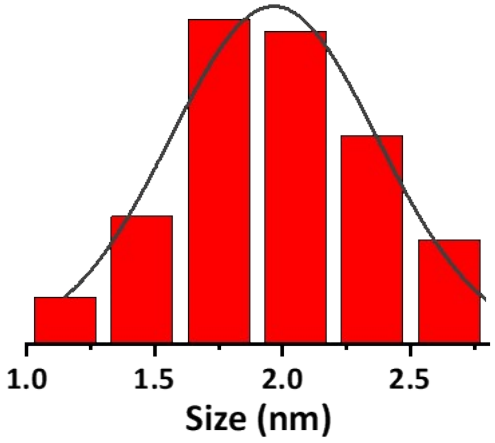

Figure S1. Size distribution histogram of CDs.

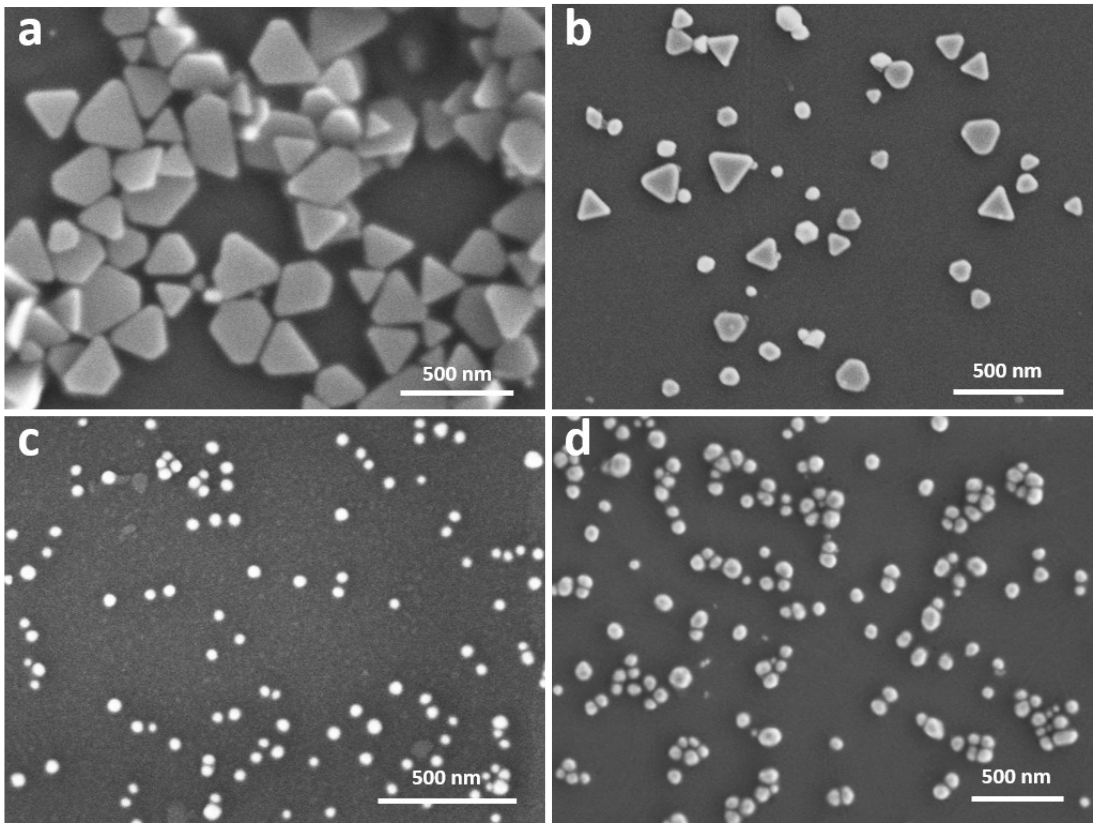

Figure S2. SEM images of prepared AgNPs, CDs/Ag-5, CDs/Ag and CDs/Ag-15.

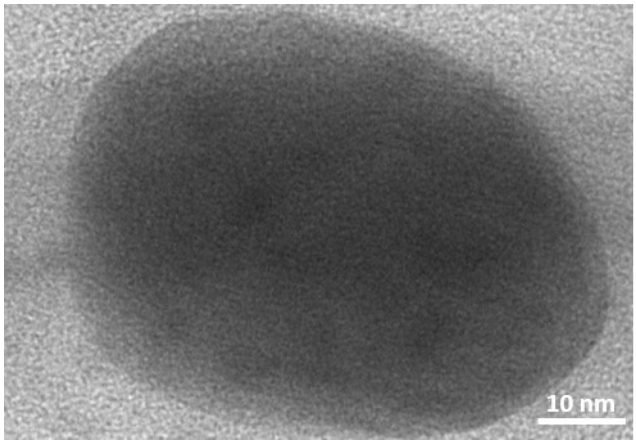

Figure S3. TEM image of prepared CDs/Ag.

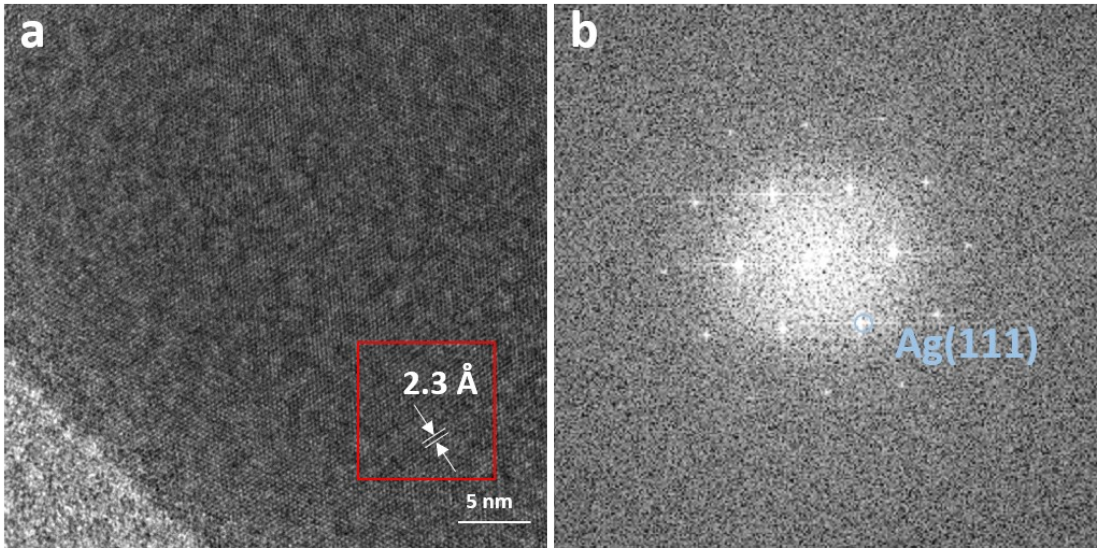

Figure S4. (a) HRTEM image and (b) the corresponding FFT pattern of Ag NPs.

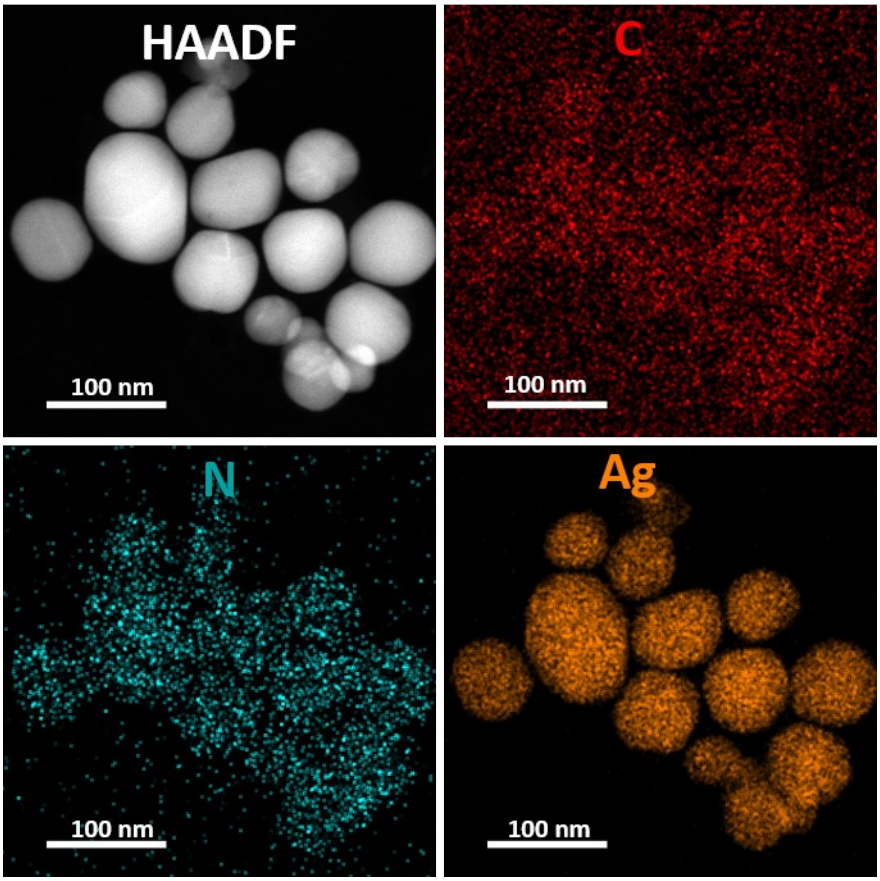

Figure S5. STEM-EDX mapping images of CDs/Ag in large field of view.

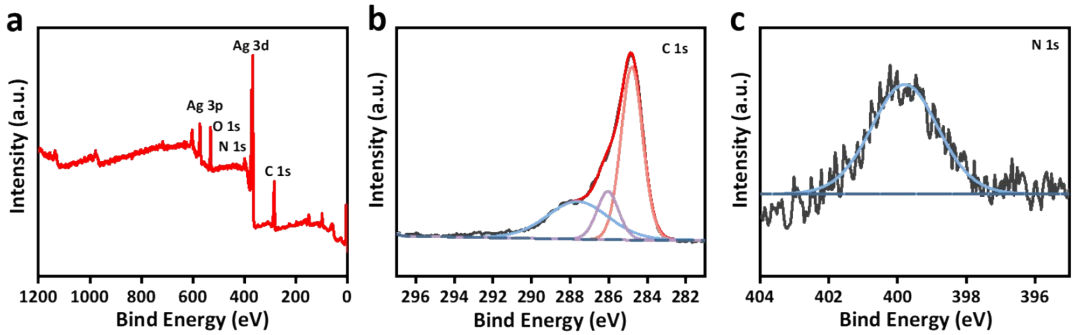

Figure S6. (a) XPS survey spectra, (b) C 1s and (c) N 1s XPS spectrum of CDs/Ag.

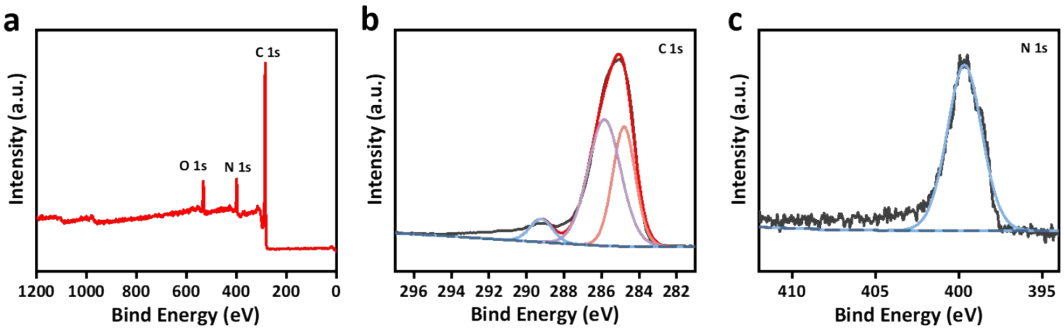

Figure S7. (a) XPS survey spectra, (b)C 1s and (c) N 1s XPS spectrum of CDs.

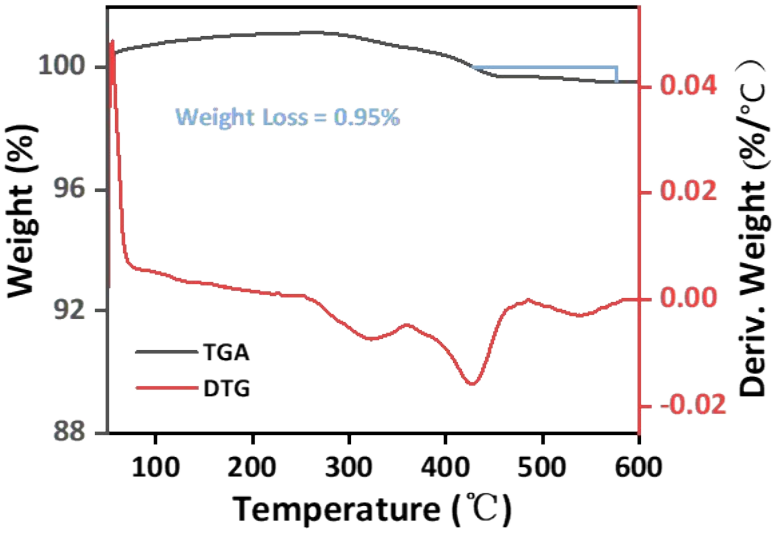

Figure S8. TGA and DTG curve of Ag NPs.

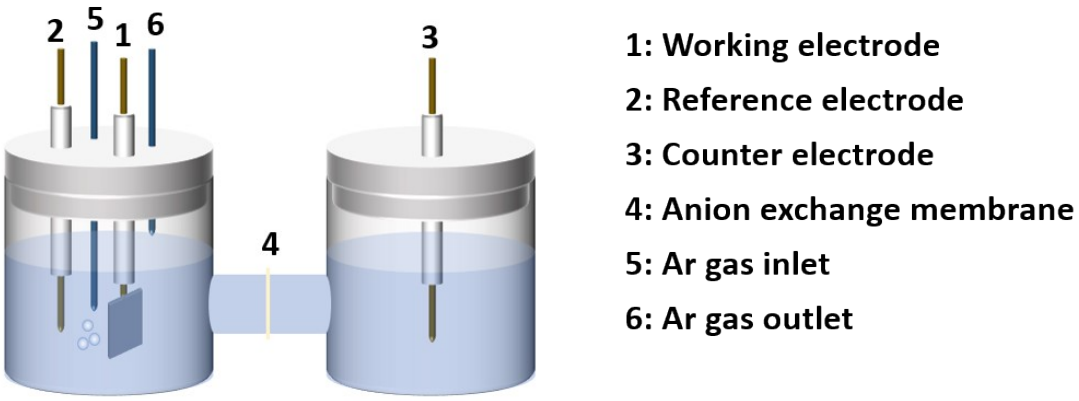

Figure S9. H-cell electrolytic cell for NO_3RR.

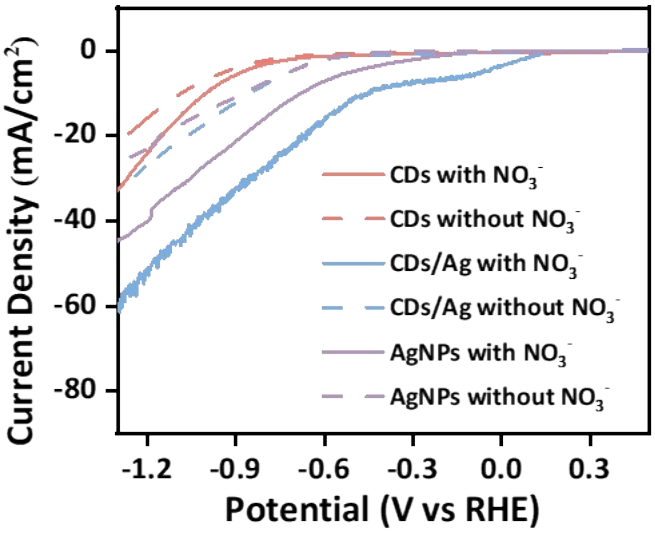

Figure S10. LSV curves of CDs, AgNPs and CDs/Ag in 0.1 M KOH with and without 0.1 M KNO_3.

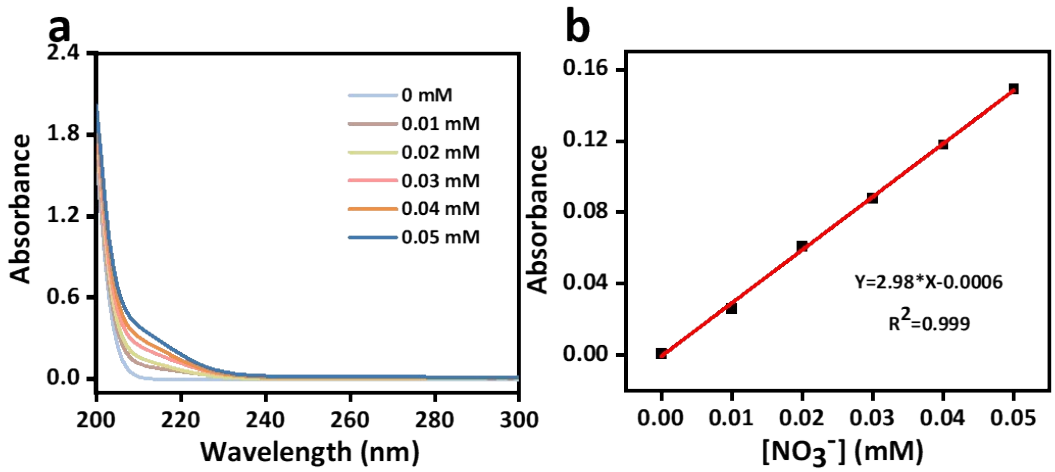

Figure S11. (a) The ultraviolet-visible absorption spectra of KNO_3 solution with different NO_3^- concentrations. (b) The linear standard curve for the calculation of NO_3^-.

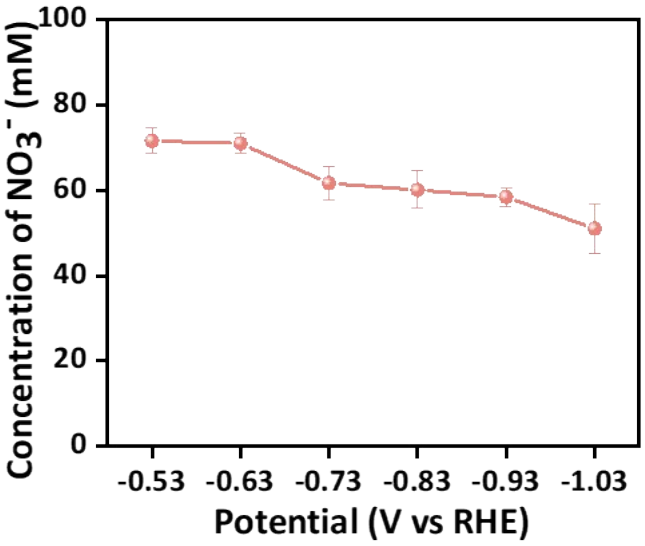

Figure S12. The concentration and conversion of NO_3^- over CDs/Ag ranging from -0.53 to -1.03 V vs RHE.

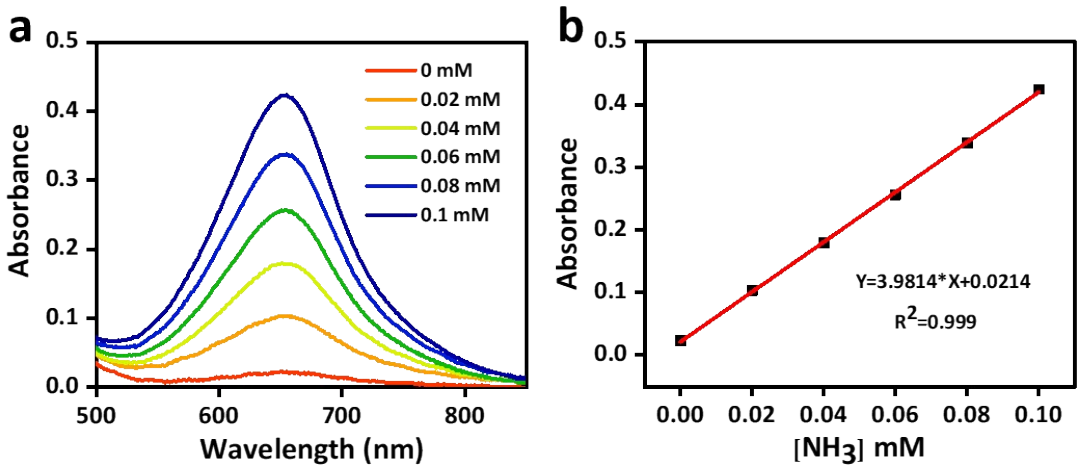

Figure S13. (a) The ultraviolet-visible absorption spectra of NH_4Cl solution with different ammonia concentrations. (b) The linear standard curve for the calculation of ammonia production.

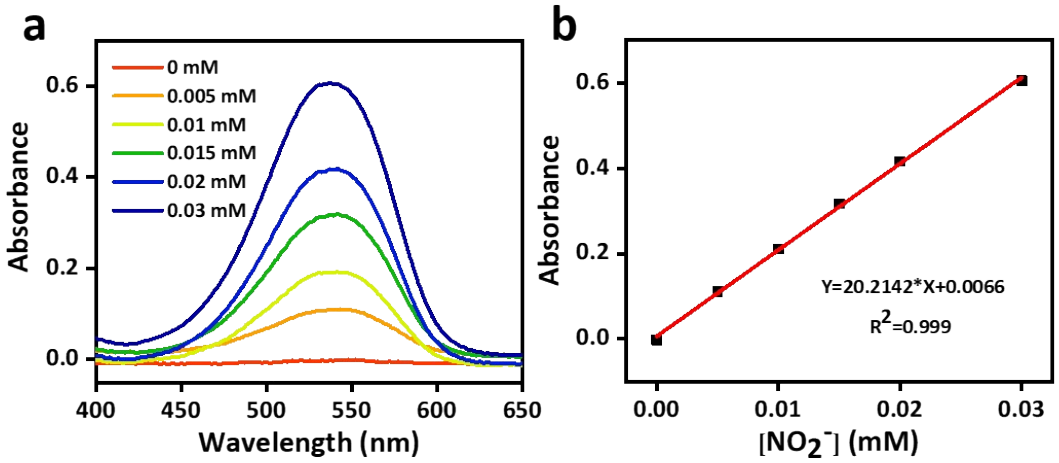

Figure S14. (a) The ultraviolet-visible absorption spectra of KNO_2 solution with different concentrations. (b) The linear standard curve for the calculation of NO_2^- production.

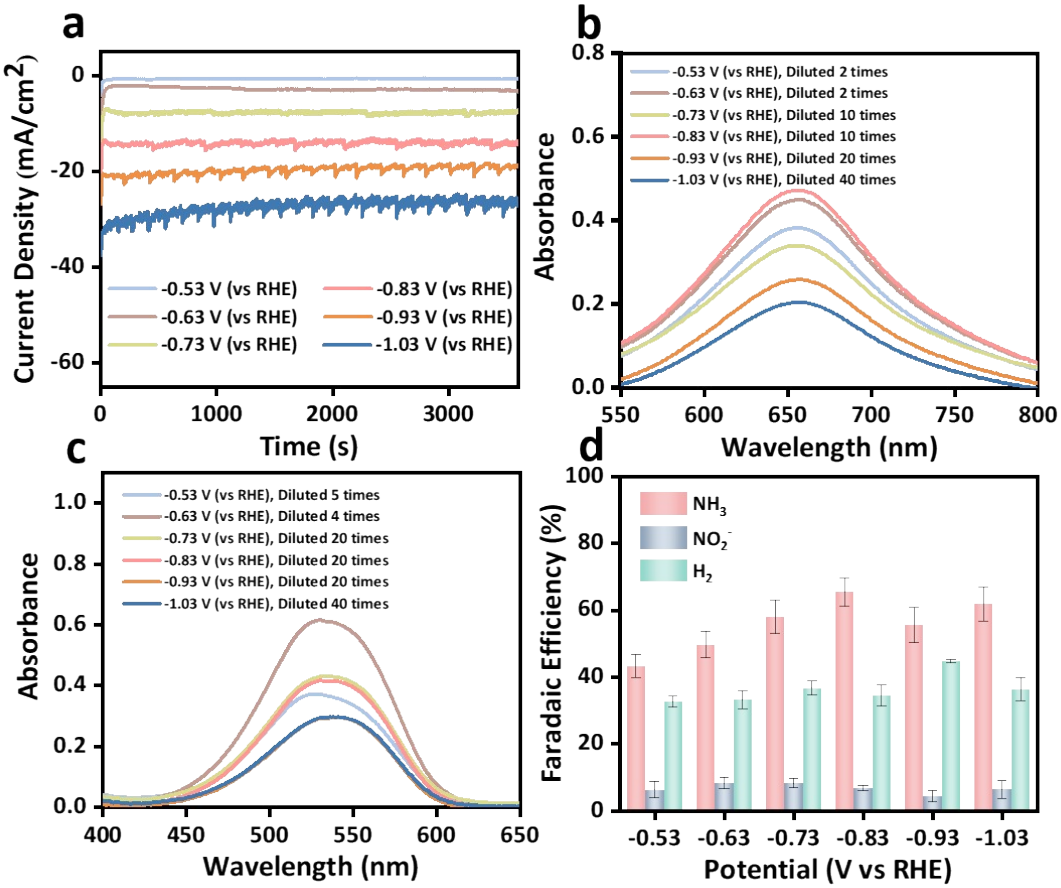

Figure S15. (a) Chronoamperometry curves of CDs at various potentials for 1 h in 0.1 M KOH and 0.1 M KNO_3. (b) UV-Vis absorption spectra of NH_4^+ after 1 h electrolysis of CDs at various potentials. (c) UV-Vis absorption spectra of NO_2^- after 1 h electrolysis of CDs at various potentials. (d) Potential-dependent FE_{NH3}, FE_{NO2-} and FE_{H2} over CDs.

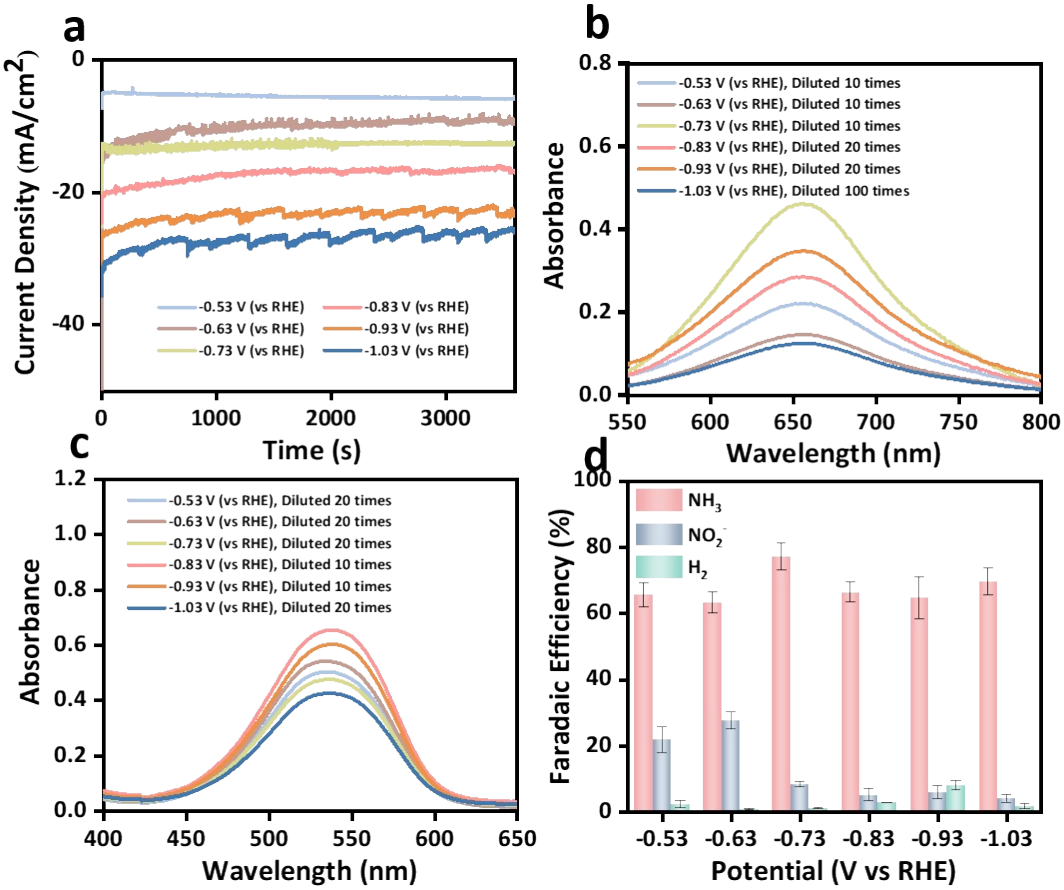

Figure S16. (a) Chronoamperometry curves of AgNPs at various potentials for 1 h in 0.1 M KOH and 0.1 M KNO_3. (b) UV-Vis absorption spectra of NH_4^+ after 1 h electrolysis of AgNPs at various potentials. (c) UV-Vis absorption spectra of NO_2^- after 1 h electrolysis of AgNPs at various potentials. (d) Potential-dependent FE_{NH3}, FE_{NO2-} and FE_{H2} over AgNPs

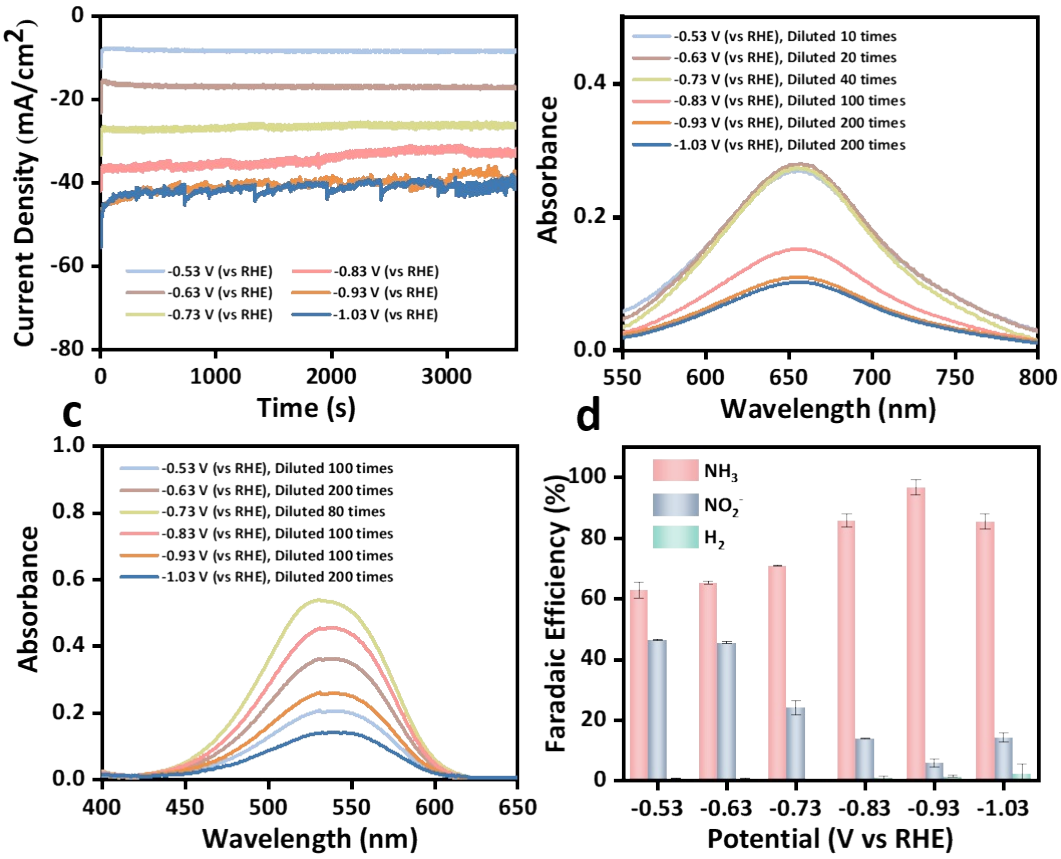

Figure S17. (a) Chronoamperometry curves of CDs/Ag at various potentials for 1 h in 0.1 M KOH and 0.1 M KNO_3. (b) UV-Vis absorption spectra of NH_4^+ after 1 h electrolysis of CDs/Ag at various potentials. (c) UV-Vis absorption spectra of NO_2^- after 1 h electrolysis of CDs/Ag at various potentials. (d) Potential-dependent FE_{NH3}, FE_{NO2-} and FE_{H2} over CDs/Ag.

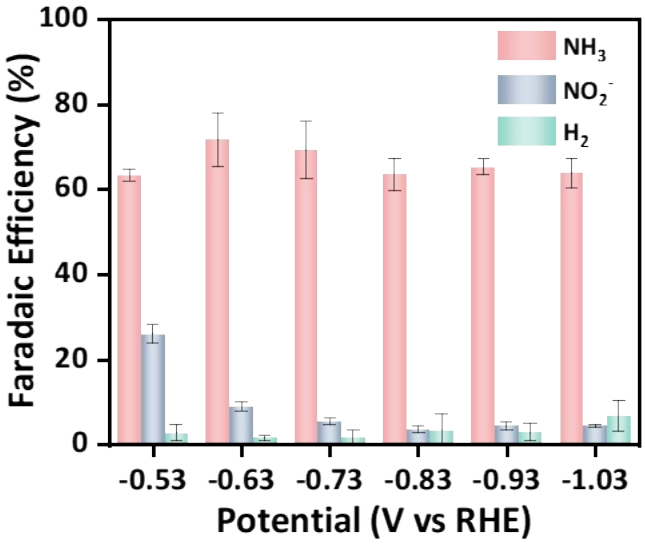

Figure S18. Potential-dependent FE_{NH3}, FE_{NO2-} and FE_{H2} over CDs/Ag-5.

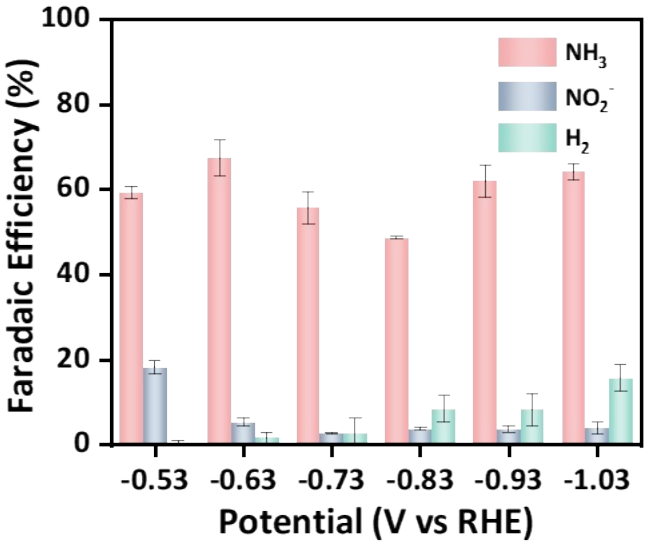

Figure S19. Potential-dependent FE_{NH3}, FE_{NO2-} and FE_{H2} over CDs/Ag-15.

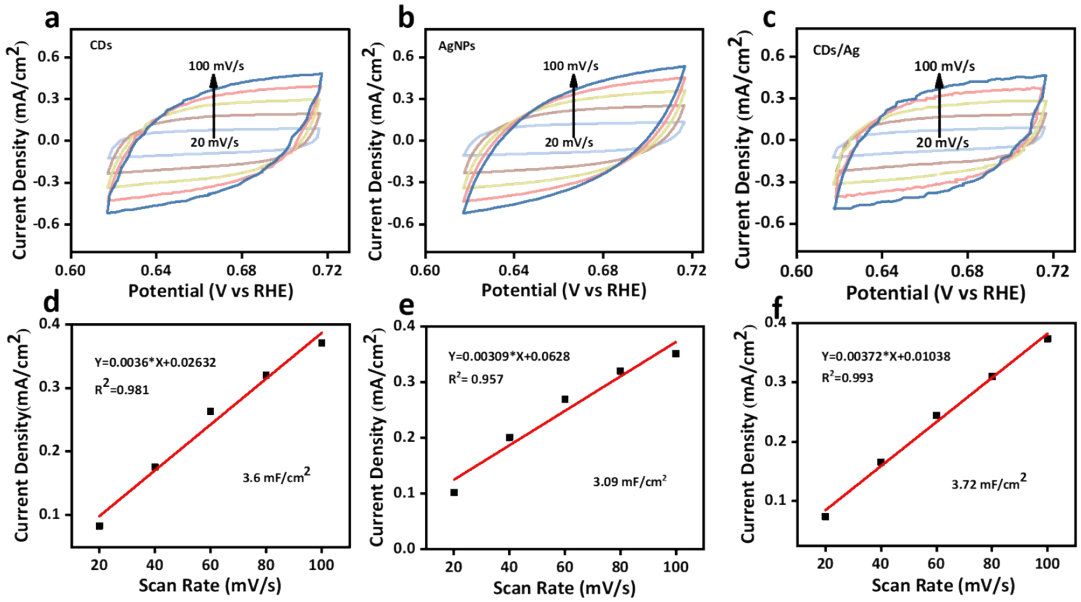

Figure S20. ECSA measurements of the CDs, AgNPs and CDs/Ag. (a, b, c) The cyclic voltammetry profiles obtained on the CDs, AgNPs and CDs/Ag at the sweep rates 20, 40, 60, 80, 100 mV/s, respectively. (d, e, f) The determination of double layer capacitance for each catalyst.

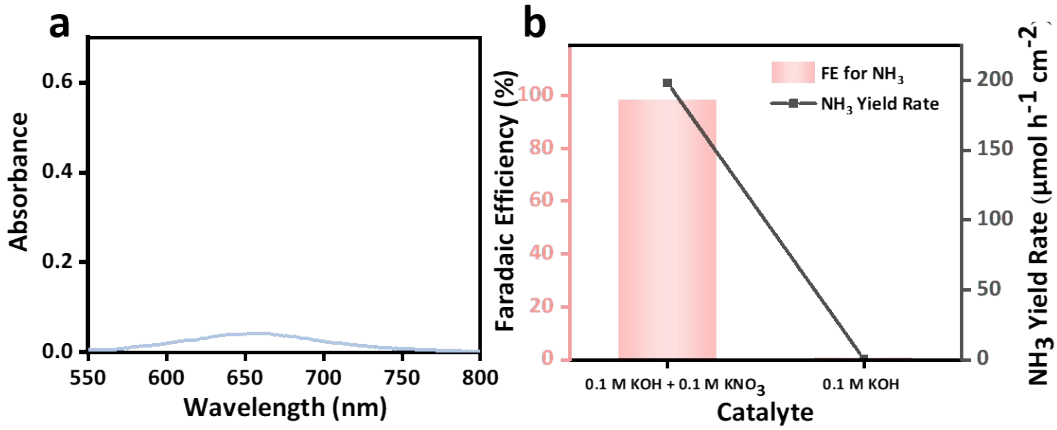

Figure S21. (a) UV-Vis absorption spectra of NH_4^+ after 1 h electrolysis of CDs/Ag in 0.1 M KOH. (b) The FE_{NH3} and Y_{NH3} over CDs/Ag in 0.1 M KOH with and without 0.1 M KNO_3.

Table S1 Comparison of NO_3RR performance in reported literature.

Catalysts	Electrolyte	Potential (V vs RHE)	Faradaic efficiency of NH_3	Yield rate of NH_3 ($\mu mol\ h^{-1}\ cm^{-2}$)	Ref.
CDs/Ag	0.1 M KOH+0.1 M KNO_3	-0.93	98.48%	198.12	This work
Fe SAC	0.1 M KOH+0.1 M KNO_3	-0.7	98%	161.76	1
PTCDA/O-Cu	0.1 M PBS + 500 ppm NO_3	-0.4	85.9%	25.64	2
Cu_3P NA/CF	0.1 M PBS +0.1 M $NaNO_3$	-0.5	91.2%	95.68	3
Cu@CuHHTP	0.5 M Na_2SO4+500 ppm NO_3^-	-0.9	67.55%	108.23	4
Cu-Pd/C nanobelts	0.1 M KOH+0.01 M KNO_3	-0.4	62.3%	12.98	5
CuOx nanoparticles	0.1 M KOH+0.1 M KNO_3	-0.25	74.18%	26.41	6
Cu/Cu2O	0.5 M Na_2SO4+500 ppm NO_3^-	-0.85	95.8%	244.9	7
Cu nanosheets	0.1 M KOH+0.01 M KNO_3	-0.15	99.7%	22.94	8
Ir NTs	0.1 M HClO4+1 M NaNO3	0.06	84.7%	54.17	9
Cu-N-C SAC	0.1 M KOH+0.1 M KNO_3	-0.1	84.7%	260	10

References

1 P. P. Li, Z. Y. Jin, Z. W. Fang and G. H. Yu, *Energy Environ. Sci.*, 2021, **14**, 3522–3531.
2 Gao-Feng Chen, Yifei Yuan, Haifeng Jiang, Shi-Yu Ren, Liang-Xin Ding, Lu Ma, Tianpin Wu, Jun Lu and Haihui Wang, *Nat. Energy*, 2020, **5**, 605–613.
3 Jie Liang, Biao Deng, Qin Liu, Guilai Wen, Qian Liu, Tingshuai Li, Yonglan Luo, Abdulmohsen Ali Alshehri, Khalid Ahmed Alzahrani, Dongwei Ma and Xuping Sun, *Green Chem.*, 2021, **23**,5487–5493.
4 Xiaojuan Zhu, Haicai Huang, Huaifang Zhang, Yu Zhang, Peidong Shi, Kaiyu Qu, Shi-Bo Cheng, An-Liang Wang and Qipeng Lu, *ACS Appl. Mater. Interfaces*, 2022, **14**, 32176−32182.
5 Zhe Wang, Congcong Sun, Xiaoxia Bai, Zhenni Wang, Xin Yu, Xin Tong, Zheng Wang, Hui Zhang, Haili Pang, Lijun Zhou, Weiwei Wu, Yanping Liang, Ajit Khosla and Zhenhuan Zhao, *ACS Appl. Mater. Interfaces*, 2022, **14**, 30969–30978.
6 Jing Geng, Sihan Ji, Hui Xu, Cuijiao Zhao, Shengbo Zhang and Haimin Zhang, *Inorg. Chem. Front.*, 2021, **8**, 5209–5213.
7 Yuting Wang, Wei Zhou, Ranran Jia, Yifu Yu and Bin Zhang, *Angew. Chem. Int. Ed.*, 2020, **59**, 5350–5354.
8 Xianbiao Fu, Xingang Zhao, Xiaobing Hu, Kun He, Yanan Yu, Tao Li, Qing Tu, Xin Qian, Qin Yue, Michael R. Wasielewski and Yijin Kan, *Appl. Mater. Today*, 2020, **19**, 100620.
9 Ranran Jia, Yuting Wang, Changhong Wang, Yangfang Ling, Yifu Yu and Bin Zhang, *ACS Catal.*, 2020, **10**, 3533–3540.
10 Ji Yang, Haifeng Qi, Anqi Li, Xiaoyan Liu, Xiaofeng Yang, Shengxin Zhang, Qiao Zhao, Qike Jiang, Yang Su, Leilei Zhang, Jian-Feng Li, Zhong-Qun Tian, Wei Liu, Aiqin Wang and Tao Zhang, *J. Am.Chem. Soc.*, 2022, **144 (27)**, 12062-12071.